



City Research Online

City, University of London Institutional Repository

Citation: Zhang, Z., Li, Q., Bruecker, C. & Zhang, Q. (2022). Enhanced Thermal Performance with High-Amplitude Intermittent Impingement Cooling. *International Journal of Heat and Mass Transfer*, 185, 122359. doi: 10.1016/j.ijheatmasstransfer.2021.122359

This is the accepted version of the paper.

This version of the publication may differ from the final published version.

Permanent repository link: <https://openaccess.city.ac.uk/id/eprint/27215/>

Link to published version: <https://doi.org/10.1016/j.ijheatmasstransfer.2021.122359>

Copyright: City Research Online aims to make research outputs of City, University of London available to a wider audience. Copyright and Moral Rights remain with the author(s) and/or copyright holders. URLs from City Research Online may be freely distributed and linked to.

Reuse: Copies of full items can be used for personal research or study, educational, or not-for-profit purposes without prior permission or charge. Provided that the authors, title and full bibliographic details are credited, a hyperlink and/or URL is given for the original metadata page and the content is not changed in any way.

City Research Online:

<http://openaccess.city.ac.uk/>

publications@city.ac.uk

Enhanced Thermal Performance with High-Amplitude Intermittent

Impingement Cooling

Zhihan Zhang⁽¹⁾, Qianhui Li⁽²⁾, Christoph Bruecker⁽²⁾, Qiang Zhang^{(1,2)*}

⁽¹⁾ University of Michigan – Shanghai Jiao Tong University Joint Institute,
Shanghai Jiao Tong University, Shanghai, China

⁽²⁾ City, University of London, London, UK

* Corresponding author: qzhang@sjtu.edu.cn

Abstract:

The advances of many future engineering applications rely on effective cooling techniques. Beyond the traditional thermal management solutions, the design potential of unsteady impingement cooling is still under-explored. As a combined experimental and numerical study, this paper reports new findings on high-amplitude intermittent impingement cooling with controlled unsteady patterns. Specific attention was paid on the intermittent flow close time ratio. The experimental work involved unsteady cooling performance measurement with a small-scale water tunnel system. Unsteady Reynolds Averaged Navier-Stokes Simulation (URANS) was conducted to illustrate the unsteady flow physics, and to evaluate the cooling performance at a wider range of flow conditions (average Reynolds number $2800 < Re_m < 10000$, pulsating frequency $0.1 \text{ Hz} < f < 2 \text{ Hz}$, close time ratio $0.2 < \gamma < 0.8$). Both experimental and numerical data confirm a remarkable improvement of overall cooling efficiency by high-amplitude intermittent impingement flow. Especially around the wall jet region, the enhancement can reach as high as 50%. The generation and interaction of vortex rings break the development of thermal boundary layer, and enhance the generation of near wall turbulence, especially for the wall jet region. Saving in coolant consumption with high-amplitude intermittent impingement cooling technique in practice is also demonstrated. The novel concept presented in this paper can be applied to a wide range of applications including electronic cooling, deicing, gas turbine blade cooling, etc.

Key words: Impingement cooling, intermittent, conjugate heat transfer, vortex rings

Nomenclature

Roman symbols		t	Flow time, (s)
Bi	Bior number, $\frac{hL}{k_s}$	Subscripts	
Fo	Fourier number, $\frac{\alpha t_{period}}{L^2}$	0	Stationary point
Nu	Nusselt number, $\frac{hD}{k_l}$	ave	Integral average value, range: $r/D = 0 \sim 6$
Re	Reynolds number, $\frac{\rho U_m D}{\mu_w}$	s	Solid
D	Inner Diameter of inlet pipe, (mm)	l	Liquid
f	Pulsating frequency, (Hz)	m	Time averaged value
H	Height from pipe exit to plate, (mm)	∞	Incoming flow
H_{add}	Extra height in simulation domain, (mm)	Greek symbols	
h	heat transfer coefficient, ($W \cdot m^{-2} \cdot K^{-1}$)	α	Thermal diffusivity, ($m^2 \cdot s^{-1}$)
k	Heat conductivity, ($W \cdot m^{-1} \cdot K^{-1}$)	γ	Close time ratio, $\frac{\text{close time}}{\text{period}}$
L	solid thickness, (mm)	δ	Relative difference between steady and unsteady results, (%)
q_{CHT}	Constant heat flux at solid side, ($W \cdot m^{-2}$)	η_{CHT}	conjugate cooling efficiency, $\frac{q_{\text{CHT}} D}{(T_{\text{CHT}} - T_{\infty}) k_s}$
r	Radial distance, (mm)	$\delta \bar{\eta}_{\text{CHT}}$	Area-averaged integral difference of cooling efficiency, (%)
T_{CHT}	Temperature at solid side, ($^{\circ}C$)	μ_w	Water dynamic viscosity, ($Pa \cdot s$)
T_{Conv}	Temperature at fluid-solid interface, ($^{\circ}C$)	ω_z	Z direction vorticity, (s^{-1})

1. Introduction

Impingement cooling is one of the most effective thermal management techniques widely employed in gas turbine cooling, electronic cooling, manufacturing process, etc. There have been continuous research efforts to explore the design space and potential of this technique to meet the ever-growing cooling demand in various industries.

Steady impingement cooling has been widely investigated during the past decades. The key flow characteristics identified involve potential core region, initial free jet region, decaying jet region, stagnation region and wall jet region^[1]. Correspondingly, steady jet impingement cooling is very effective near the stagnation region, but the thermal performance drops rapidly with the growing boundary layers downstream of the wall jet region. The Nusselt number profile shows a typical saddle-shaped distribution with a secondary peak at around $r / D = 2$ ^[2]. The reasons are attributed to either the transition from laminar flow to turbulent flow^[3], enhancement of turbulent intensity^[4] or the vortex dynamics in the boundary layers^[5].

It has been recognized that unsteady jet impingement has the potential to enhance heat transfer by the introduction of boundary layer break-up and renewal mechanism^[6]. Figure 1 shows different unsteady patterns of impingement jet studied in the open literatures. Oscillating jet refers to zero mean flow rate, while Pulsating jet has a non-zero mean flow rate. Different periodic variation patterns of the jet inlet flow have been studied, including sinusoidal^[7,8], square^[9,10] or intermittent pulsating waves^[11].

Pulsating amplitude and frequency are the important control variables considered in the unsteady impingement cooling studies. Behera et al.^[12] found that enhancement in time-averaged Nusselt number can be achieved by the augmentation of freestream turbulence when the pulsating amplitude is strong enough. A 35% enhancement was observed in the wall jet region when the pulsating amplitude reaches over 40% ($5130 < Re < 8156$). For a higher range of Reynolds numbers ($14000 < Re < 78000$), Hofmann et al.^[13] show that heat transfer enhancement varies from 3.5% to 30% with the increase

of amplitude. The effect of pulsating frequency is more complex. Results from Hofmann et al.^[13] indicate the trend strongly depends on the geometry setup. Some studies showed that there is a threshold of frequency^[13,14], beyond which heat transfer can be enhanced with the increase of frequency and amplitude^[15]. Studies by Mladin et al.^[14] suggest the threshold of Strouhal number is 0.26. Esmailpout et al.^[15] report a maximum increase of 28% beyond this threshold ($Re = 5500, 60 < f < 350$ Hz). In contrast, heat transfer enhancement under this threshold was also reported by other studies^[11,16]. Li et al.^[16] conclude that the optimal Strouhal number increases with Reynolds numbers ($10000 < Re < 20000$), and ranges between 0.24 and 0.48. There are still many inconclusive and at times conflicting findings in the open literature: the thermal performance can be either increased^[17-20], declined^[7,13,21] or no marked influence^[8,16].

The square pulsation mode shown in Fig. 1 has been found to have better enhancement in heat transfer than the sinusoidal pulsating pattern^[7,22,23]. Practically, square waveforms were approximately realized by solenoid control valve or rotating wheel in these studies. The experiments results by Sheriff et al.^[7] show the time-averaged stagnation Nusselt number decreases 17% with the sinusoidal wave, but increases 33% with the square wave ($3000 < Re < 20000, 60 < f < 280$ Hz). Xu et al.^[8,9] indicate that the intermittent pulsation can effectively enhance the heat transfer than the other pulsating patterns due to higher turbulence and larger vortices introduced ($1820 < Re < 8000, 33 < f < 67$ Hz). The study by Li et al.^[10] demonstrates that triangular wave is more beneficial for heat transfer enhancement instead of square wave when the net mass flow rate is zero, especially at higher frequency ($10000 < Re < 20000, 10 < f < 30$ Hz).

An important control parameter for intermittent impingement cooling is the time ratio between jet opening and close time. There has been very limited attention for this time ratio among most of the existing studies. Sailor et al.^[11] report improved thermal performance associated with lower duty cycle (cycle on time to total cycle), and more than 50% enhancement in stagnation region with the optimal combination of amplitude and frequency ($21000 < Re < 31000, 20 < f < 60$ Hz).

In practice, the allowable jet opening and close time ratio is directly related to the solid heat diffusion process. Compared to convection, the conduction in the solid is a much slower process. The disparity in time scales could be up to a few orders of magnitudes^[24], which also means there is a significant time delay for an intermittent flow to leave a thermal signature on the hot-end of a solid. With the solid “thermal buffer” as an additional control variable, a longer time interval between two adjacent intermittent jets (lower duty cycle or longer close time shown in Fig.1) can be allowed in practice.

The design space for intermittent impingement cooling with high-amplitude has not been well explored so far. To the authors’ knowledge, no conjugate intermittent impingement cooling measurement data (at high “close time ratio”) have been published in the open literature. This paper reports new experimental and numerical findings on intermittent impingement cooling performance at various frequencies ($0.1 \text{ Hz} < f < 2 \text{ Hz}$) and close time ratios ($0.2 < \gamma < 0.8$). The novel concept and potential benefit of high amplitude intermittent cooling is firstly demonstrated by 1D unsteady conjugate heat transfer analysis, then further illustrated by full-scale Unsteady Reynolds Averaged Navier-Stokes Simulation (URANS). Typical flow conditions in electronic cooling were employed (average Reynolds number $2800 < Re_m < 10000$). The experimental work involves unsteady cooling performance measurement with a small-scale water tunnel system. After validation of the numerical model, the unsteady flow physics and the cooling performance at a wider range of flow conditions are discussed. Further practical potential benefit of intermittent impingement cooling at high close time ratio is demonstrated in the end.

2. 1D Unsteady Conduction Analysis

The potential benefit of high-amplitude intermittent impingement cooling can be conceptually demonstrated by 1D finite difference analysis of conduction with an arbitrarily assumed unsteady convection boundary condition.

Figure 2(a) presents a simplified model for an electrical cooling process, where the temperature at the heating end T_{CHT} is the control objective. A constant heat flux q is applied to a solid with characteristic thickness L . Heat is convected away on the other side with time-varying convective heat transfer coefficient $h(t)$ and a constant incoming temperature T_{∞} . A Forward Time Central Space (FTCS) method was employed to solve the 1D energy equation with a time-varying convection boundary conditions listed as follows:

$$\frac{\partial T}{\partial t} = \alpha \frac{\partial^2 T}{\partial x^2} \quad (1)$$

$$-k \frac{\partial T}{\partial x} \Big|_{x=0} = q \quad (2)$$

$$-k \frac{\partial T}{\partial x} \Big|_{x=L} = h(t)(T_{\text{Conv}}(t) - T_{\infty}) \quad (3)$$

For an unsteady intermittent cooling process shown in Fig. 1, the close time ratio is defined as:

$$\gamma = \frac{\text{close time}}{\text{period}} \quad (4)$$

Due to the thermal capacity of the solid material, there is a significant time delay between the temperature at the heating end T_{CHT} and the temperature at the convection side T_{Conv} , which means in practice a higher close time ratio γ for an intermittent cooling process can be allowed without concerning the overheating issue at the heating end. Here, a frequency of 0.1 Hz (corresponding Fourier number Fo of 40) and a high close time ratio of 0.8 were selected to demonstrate the concept of intermittent cooling process.

In practice, with the same amount of averaged cooling supply, a high close time ratio for intermittent flow means re-distributing the same cooling flow into a short time. An improved convection rate (higher $h(t)$) is expected with the higher Reynolds number during the short flow opening time. It remains unclear exactly how much short-term enhancement is required (or can be achieved in practice), so that an overall time-averaged performance benefit can be obtained. This will be further addressed in the numerical and experimental work discussed later. In this 1D concept demonstration process, the convective heat transfer coefficient was arbitrarily assumed to be six times

of the steady cooling condition.

Figure 2(b) illustrates the Biot number variations during the unsteady conjugate heat transfer process. The temperature histories of nondimensional temperature T_{CHT} and T_{Conv} are compared with solutions for a steady cooling process. For the intermittent cooling case, both T_{CHT} and T_{Conv} are lower than the steady result. There is a significant phase lag between temperature histories at both ends of the solid: right after the stop of cooling, the increase of T_{Conv} is associated with decrease of T_{CHT} . The disparity in time scales between conduction and convection causes such time delay. Such thermal buffering effect by the solid material allows a longer close time for jet impingement.

For intermittent cooling, accurate estimation of the short-period enhancement in convective heat transfer and the overall performance benefit requires full-scale unsteady CFD simulations as well as experimental validation, which will be presented next.

3. CFD methods and validation

Figure 3(a) shows an axisymmetric computational domain for the present study. The key dimensions are the same as used in the configurations from Alimohammadi et al.^[25] for a typical electronic cooling application. The distance from the incoming jet to the target plate is the same as the inner diameter D (13 mm) of the inlet pipe. The dimensions of the flow domain were selected as $16D \times 4D$ to ensure the development of an unconfined and submerged jet^[26]. The solid domain is aluminum material with a thickness of $0.4D$ (5 mm). A constant heat flux q (130 kW/m^2) is applied to the solid external boundary.

To simplify the computation domain and keep the consistent inlet boundary conditions with the experimental setup, a separate CFD simulation at the same Reynolds number for a pipe flow with a length of $32D$ was conducted. The resulting exit velocity profile was then mapped to the inlet of the computational domain using User Defined Function (UDF). Similar inlet boundary condition setup method was also

employed by Alimohammadi et al.^[25].

Figure 3(b) provides the temporal fluctuation history of the normalized jet Reynolds number based on the averaged velocity at the inlet. A transition slope was added to the pulsation profile to avoid the sudden step change. The cycle mean jet Reynolds number (overall flow rate) was kept the same for both steady and unsteady conditions. Therefore, the pulsation amplitude is determined by the close time ratio γ (for instance, $Re/Re_m = 5$ when $\gamma = 0.8$). The cycle mean jet Reynolds numbers range from 2800 to 10000, which are the typical values among existing electronic cooling studies^[25,27,28].

All cases were calculated under fully turbulent condition. Transition with SST turbulence model was selected due to its prediction performance recognized by other studies^[1,29]. The model is based on two transport equations, one for intermittency and one for a transition onset criterion in terms of momentum thickness Reynolds number (Langtry et al.^[30]). Simple algorithm was adopted, and pressure, momentum and energy terms were calculated based on second-order upwind formula.

Structured mesh was employed, and the near wall y^+ is less than 1 to resolve the boundary layer development^[30]. Results of grid independence study are shown in Fig. 4. The Nusselt numbers at the stagnation point location and the area integral-averaged value ($0 < r/D < 6$) are quantitatively compared. The difference between the results of 66K and 215K grids is negligible. Therefore, the mesh with 66K grids size was employed for the steady and unsteady calculations presented in this paper.

Figure 5 shows the Nusselt number distributions from steady CFD computations compared to previous experimental and numerical data by Alimohammadi et al.^[25]. In general, the agreement is satisfactory. The simulation data fit well at $r/D > 1$ and the discrepancies are within the uncertainty range of the experimental data. Major deviation occurs at the stagnation region mostly due to the limited information available for the inlet velocity profile in the previous experimental study^[25].

Unsteady Reynolds-Averaged Navier-Stokes (URANS) calculation was conducted for the intermittent impinging flow. All unsteady computations were initialized from a steady run. The numerical time step was adjusted based on the pulsating frequency. The temperature values at the stagnation point location and area

integral-averaged value are also quantitatively monitored to check the sensitivity of time step selected. The maximum error is less than 0.5%.

The frequency and close time ratio studied are in the range of $0.1\text{Hz} \leq f \leq 2\text{ Hz}$, $0.2 \leq \gamma \leq 0.8$, respectively.

To evaluate the overall thermal performance, the cooling efficiency η_{CHT} is defined as:

$$\eta_{\text{CHT}} = \frac{q_{\text{CHT}}D}{(T_{\text{CHT}} - T_{\infty})k_s} \quad (5)$$

where T_{CHT} and q_{CHT} are the temperature and heat flux at the heating end, respectively, and k_s is the thermal conductivity of the solid material.

In this paper, only time-averaged cooling efficiency data are presented. The differences between steady and unsteady conditions are evaluated under the same mean Reynolds numbers.

4. Experimental rig and measurement method

Figure 6 shows the experimental setup employed in the present study. Water flow was driven by a centrifugal pump in a close-loop circuit. A gate valve was used to prevent backflow and to control the flow rate. Various pulsation patterns were controlled by a diaphragm solenoid valve, driven by the voltage signal generated from NI Data Acquire System (DAQ). The response time of the solenoid valve is 20ms. The instantaneous volume flow rate was recorded by a Noike flow meter.

In the test section, water jet was initiated from a pipe with a sharp edge at the exit. The pipe has a total length of $32D$ to ensure a fully developed entry velocity profile, and a consistency with the CFD simulation. The distance between the pipe exit and the heating plate is same as the pipe diameter. A double layer cylindrical test chamber was used to provide a uniform axisymmetric overflow at the exit chamber.

An aluminum plate with thickness of 5 mm was heated on the lower surface by using a Polyimide (PI) film electric heater. The heater was insulated with high silicon

oxygen fiberglass to minimize external heat loss. The heat loss calculated according to insulation surface temperature is less than 1% of the total heat load and can be neglected. Four T-type thermocouples were embedded between the plate and film heater at location $r / D = 2\sim 5$ with a constant spacing D . The limited number of thermocouples employed in the measurement was due to the technical difficulties caused by the small-scale test model.

A series of intermittent impingement cooling measurements were conducted at a mean jet Reynolds number of 2800 and close time ratios ($0.2 < \gamma < 0.8$). Only low frequency condition (0.1 Hz) was considered in the present conjugate heat transfer measurement. There are two reasons. Firstly, as discussed previously, the slow thermal diffusion process can allow a reasonably long intermittent cooling “close time” without the overheating concern in electronic cooling application. A higher pulsating frequency would not make the best use of the “buffer time” offered by the conduction process. Secondly, due to controllability of the cooling water system (similar scenario as the practical electronic cooling application), it was difficult to achieve a higher frequency in the present experimental study.

Figure 7 shows the jet Reynolds number fluctuations recorded during the real-time intermittent impingement cooling tests with mean jet Reynolds number of 2800. Due to practical issues related with signal time delay, valve performance, and fluid settling time, the ideal intermittent impingement patterns used in the numerical study shown in Fig.3(b) cannot be accurately reproduced (similar to many other unsteady impingement cooling experimental studies)

Each unsteady cooling experiment was repeated ten times. The maximum random error of temperature is $\pm 4.7\%$ based on 95% confidence interval. Other detailed error sources are listed in Table 1. Using the error-transfer methodology^[31], the overall uncertainty of cooling efficiency is $\pm 5.0\%$.

5. Results and Discussion

In this section, the benefit of high-amplitude intermittent impingement cooling is firstly demonstrated by the experimental and numerical results at a lower frequency $f = 0.1$ Hz and mean jet Reynolds number of 2800. The flow physics revealed by the numerical study is discussed next, together with results at a wider range of pulsating frequencies and Reynolds numbers. The practical benefit of unsteady conjugate heat transfer is presented in the end. The overall cooling flow rate was kept the same for all unsteady and steady conditions.

Distributions of cooling efficiency for steady and intermittent impingement cooling at various close time ratios are shown in Fig. 8. Both experimental data and numerical results show a rather consistent trend. The radial location $r/D = 2$ is a pivot point, where the cooling efficiencies for all different conditions are similar. Within the stagnation region $0 < r/D < 2$, the unsteady cooling efficiency is lower compared with steady condition. Lower local cooling performance is associated with higher close time ratio. The second thermal peak shown in Fig. 5 cannot be observed from the overall cooling efficiency distribution due to the conduction effect along the radial direction. The significant benefit of intermittent cooling can be observed at the wall jet region ($r/D > 2$). Further away from the stagnation region, higher close time ratio consistently leads to a better cooling performance. The over-cooling at stagnation region and fast decay of thermal performance at wall jet region for steady impingement cooling can be greatly improved with the intermittent cooling pattern.

Figure 9 presents the percentage improvement of local cooling efficiency experimentally obtained at a wider range of close time ratios ($0.2 < \gamma < 0.8$). Similar to the observation in Fig. 8, a higher close time ratio is always beneficial for locations away from the stagnation region ($r/D < 2$). For location $r/D = 2$, the trend is not as clear due to the small difference at different close time ratios.

The cooling benefit shown in Figs. 8 and 9 is directly related with the enhancement of convection introduced by high-amplitude intermittent impingement flow. Based on

the further analysis by CFD simulation, two typical flow structures associated with intermittent impingement cooling are discussed next.

Figure 10 compares the streamlines and streamwise vorticity contour at the steady and intermittent cooling conditions. Results at two representative time sequences during the intermittent impingement process are presented at a close time ratio $\gamma = 0.8$ and the same mean jet Reynolds number as the experimental study ($Re_m = 2800$, $f=0.1\text{Hz}$). When the jet leaves the inlet pipe, the relative motion between jet and adjacent fluid leads to shear-layer roll-up at the trailing edge of pipe nozzle exit, which finally generates a vortex ring (note that the system is to be assumed axisymmetric). This primary vortex ring has a sense of rotation in anti-clockwise direction. After the high-pressure stagnation region, the jet accelerates along the wall, and a continuous development of the boundary layer can be observed from the steady condition. The instantaneous streamlines for the intermittent impingement case (close time ratio $\gamma = 0.8$) demonstrate the primary vortex ring generation mechanism and the evolution of a secondary vortex ring. As the primary vortex ring spreads radially, fed by the lift-up process from the boundary layer fluid below the core of the primary vortex, a secondary vortex (clockwise rotation) emerges at $r / D = 2$, as shown by the close-up view in Fig.10. The evolution of these vortices and the resulting dynamic vortex-wall interaction energizes and breaks down the boundary layer development, as evident in the vorticity contour shown in Fig. 10. The extra viscosity effect, entrainment motion and evolution of the vortex rings inevitably promote the near wall turbulence generation, which leads to the enhancement of convective heat transfer.

Figure 11 presents another vortex ring merging mechanism observed for intermittent impingement flow at a higher frequency ($f = 2 \text{ Hz}$) and higher mean jet Reynolds number ($Re_m = 10000$). Instantaneous streamlines and vorticity contours at three different time sequences are illustrated. At this higher frequency, different from the lower frequency results shown in Fig. 10, the vortex ring generated from one pulsation can catch up with the vortex from the previous pulsation cycle. Due to much stronger flow acceleration and deceleration rates, the magnitude of vorticity is higher at high pulsation frequency as well. Such a merging process of vortices from adjacent

cycles should be favorable for cooling purpose as it introduces more complex and abrupt disturbance to the near wall boundary layers.

Note that the vortex ring generation and interaction mechanism illustrated above can only provide qualitative physical explanation for the cooling enhancement associated with high-amplitude intermittent impingement cooling. Quantitatively, the URANS turbulent model employed in the present numerical might not be adequate, and still requires validation from detailed flow measurement.

Figure 12 quantitatively compares the percentage difference in cooling efficiency for different unsteady conditions, relative to results of the steady case. Both experimental and computational data at $Re_m = 2800$ and $f = 0.1\text{Hz}$ are shown in Fig. 12(a). At close time ratio $\gamma = 0.8$, there is a 15% reduction at the stagnation point location, but a remarkable augmentation of 20~30% at the wall jet region can be observed. Figure 12(b) presents the numerical result at a higher Reynolds number and higher frequency ($Re_m = 10000$ and $f = 2\text{ Hz}$). For this unsteady condition, cooling effectiveness is enhanced for all wall regions. At close time ratio $\gamma = 0.8$, a significant improvement of 50% can be observed in the wall jet region.

To evaluate the overall performance, the percentage enhancement of the area-averaged cooling effectiveness for the wall region ($0 < r / D < 6$) is shown in Fig. 13. Results at two previous intermittent conditions are compared at different close time ratios. In general, more enhancement in cooling efficiency can be observed at higher close time ratios. At close time ratio $\gamma = 0.8$, a 15% increase can be observed for the low Reynolds number low frequency case ($Re_m = 2800, f = 0.1\text{Hz}$), and a remarkable 35% enhancement can be gained at a higher Reynolds number with higher frequency ($Re_m = 10000, f = 2\text{ Hz}$)

The mean jet Reynolds numbers, or overall cooling consumption, were kept same for all the previous comparisons discussed so far. Knowing the enhancement of cooling performance by intermittent impingement, it could be useful to assess the potential benefit in coolant consumption to achieve the same allowable peak solid temperature (or cooling efficiency defined in the present study).

Figure 14 presents experimental data of cooling efficiency percentage difference

at different average Reynolds numbers ($f = 0.1\text{Hz}$, $\gamma = 0.8$). The mean jet Reynolds number of 2800 is the reference condition to calculate the percentage difference. Data for four typical locations are compared. At locations further away from the stagnation region, less coolant consumption is required to achieve the same cooling efficiency. For instance, at $r/D = 3$, a 15% reduction in coolant consumption can be observed. More saving can be gained at $r/D = 4$ and 5.

In addition to convection process, the close time ratio is also determined by the solid thermal properties (mainly diffusivity) in practical cooling applications. As demonstrated in the present study, a higher close time ratio leads to remarkable cooling benefit from the convection side. Such a higher close time ratio can only be allowed by a base material with relatively lower thermal diffusivity. In contrast with most studies in electronic cooling application, the results in this study lead to an interesting concept: materials with low thermal conductivity have the potential to provide an overall thermal benefit, and to offer more flexibility in the control of intermittent impingement cooling.

To optimize an unsteady conjugate cooling process, the list of control variables should include the solid material thermal properties, the intermittent cooling frequency, amplitude, and “close time ratio”, etc. There is an ample design space for further exploration.

6. Conclusion

This study experimentally and numerically investigated the potential benefit of high-amplitude intermittent impingement cooling. The thermal performance of steady and intermittent cooling at various mean jet Reynolds numbers ($2800 < Re_m < 10000$) and close-time ratios ($0.2 < \gamma < 0.8$) were measured in a water tunnel system. Unsteady Reynolds-Averaged Navier-Stokes calculation was conducted. Special attention was paid on the cooling performance at high close-time ratios.

Both experimental and numerical data confirm the enhancement of cooling efficiency in the wall jet region for intermittent impingement cooling at large close-time ratio. The local enhancement peak can reach 30% under low frequency and 50% under high frequency. The total area-averaged increases are 15% and 35%, separately. The more intense pulsation makes enhancement happen in larger area in wall jet region.

Further numerical analysis reveals the underlying unsteady flow physics. The generation and interaction of vortex rings, which break the development of thermal boundary layer and enhance the generation of near wall turbulence, especially for the wall jet region. The over-cooling in stagnation region and fast-decay at wall jet region for steady impingement flow can be greatly improved by intermittent cooling at higher close-time ratios.

To maintain the same allowable peak temperature, it is possible to reduce the overall coolant consumption with high amplitude intermittent cooling. In practice, solid materials with low thermal conductivity can offer more design flexibility for the optimal intermittent cooling process.

The new design space of intermittent impingement cooling demonstrated in this study can be extended to a wide range of practical applications. Further investigations should consider different ranges of scaling factors, including Reynolds number, Mach number, and Biot number used in electronic cooling, deicing, gas turbine blade cooling, etc.

Acknowledgements

The authors are grateful for the help from Dr. Hongmei Jiang and Mr. Yongmin Gu during the experimental setup. The work is sponsored by Natural Science Foundation of Shanghai (Grant number 21ZR1428800).

The 2nd and 3rd authors' time is partially supported by the EPSRC Grant Ref EP/T006315/1.

References

- [1] Zuckerman N, Lior N, Jet Impingement Heat Transfer: Physics, Correlations, and Numerical Modeling, *Advances in Heat Transfer* 39 (2006) 565-631
- [2] Lytle D, Webb B W, Air jet impingement heat transfer at low nozzle-plate spacings, *International Journal of Heat and Mass Transfer* 37 (12) (1994) 1687-97
- [3] Lee J, Lee S J, Stagnation region heat transfer of a turbulent axisymmetric jet impingement, *Experimental Heat Transfer* 12 (2) (1999) 137-156
- [4] Katti V, Prabhu S V, Experimental study and theoretical analysis of local heat transfer distribution between smooth flat surface and impinging air jet from a circular straight pipe nozzle, *International Journal of Heat and Mass Transfer* 51 (17-18) (2008) 4480-4495
- [5] Chung Y M, Luo K H, Unsteady heat transfer analysis of an impinging jet, *Journal of Heat Transfer-Transactions of the Asme* 124 (6) (2002) 1039-1048
- [6] McClelland R E. An Investigation of Convection Cooling of Small Gas Turbine Blades Using Intermittent Cooling Air[R]. U.S. Army Tank-Automotive command RD&E Center, 1988
- [7] Sheriff H S, Zumbrennen D A, Effect of flow pulsations on the cooling effectiveness of an impinging jet, *Transactions of the ASME. Journal of Heat Transfer* 116 (4) (1994) 886-95
- [8] Xu P, Mujumdar A S, Poh H J, et al., Heat Transfer Under a Pulsed Slot Turbulent Impinging Jet at Large Temperature Differences, *Thermal Science* 14 (1) (2010) 271-281
- [9] Xu P, Yu B, Qiu S, et al., Turbulent impinging jet heat transfer enhancement due to intermittent pulsation, *International Journal of Thermal Sciences* 49 (7) (2010) 1247-1252
- [10] Li P, Guo D, Liu R, Mechanism analysis of heat transfer and flow structure of periodic pulsating nanofluids slot-jet impingement with different waveforms, *Applied Thermal Engineering* 152 (2019) 937-945
- [11] Sailor D J, Rohli D J, Fu Q L, Effect of variable duty cycle flow pulsations on heat transfer enhancement for an impinging air jet, *International Journal of Heat and Fluid Flow* 20 (6) (1999) 574-580
- [12] Behera R C, Dutta P, Srinivasan K, Numerical study of interrupted impinging jets for cooling of electronics, *IEEE Transactions on Components and Packaging Technologies* 30 (2) (2007) 275-284

- [13] Hofmann H M, Movileanu D L, Kind M, et al., Influence of a pulsation on heat transfer and flow structure in submerged impinging jets, *International Journal of Heat and Mass Transfer* 50 (17-18) (2007) 3638-3648
- [14] Mladin E C, Zumbrunnen D A, Alterations to coherent flow structures and heat transfer due to pulsations in an impinging air-jet, *International Journal of Thermal Sciences* 39 (2) (2000) 236-248
- [15] Esmailpour K, Hosseinalipour M, Bozorgmehr B, et al., A numerical study of heat transfer in a turbulent pulsating impinging jet, *The Canadian Journal of Chemical Engineering* 93 (5) (2015) 959-969
- [16] Li P, Huang X Y, Guo D Z, Numerical analysis of dominant parameters in synthetic impinging jet heat transfer process, *International Journal of Heat and Mass Transfer* 150 (2020) 12
- [17] Persoons T, Saenen T, Van Oevelen T, et al., Effect of Flow Pulsation on the Heat Transfer Performance of a Minichannel Heat Sink, *Journal of Heat Transfer* 134 (9) (2012)
- [18] Raizner M, Rinsky V, Grossman G, et al., Heat transfer and flow field measurements of a pulsating round jet impinging on a flat heated surface, *International Journal of Heat and Fluid Flow* 77 (2019) 278-287
- [19] Mladin E C, Zumbrunnen D A, Nonlinear dynamics of laminar boundary layers in pulsatile stagnation flows, *Journal of Thermophysics and Heat Transfer* 8 (3) (1994) 514-523
- [20] Mladin E C, Zumbrunnen D A, Dependence of heat transfer to a pulsating stagnation flow on pulse characteristics, *Journal of Thermophysics and Heat Transfer* 9 (1) (1995) 181-192
- [21] Wang W, Gao Y, Wang G W, et al., Numerical investigation on cooling performance of pulsating flow in a ribbed channel, *Journal of Mechanical Science and Technology* 34 (4) (2020) 1765-1774
- [22] Xu P, Qiu S, Yu M, et al., A study on the heat and mass transfer properties of multiple pulsating impinging jets, *International Communications in Heat and Mass Transfer* 39 (3) (2012) 378-382
- [23] Herwig H, Middelberg G, The physics of unsteady jet impingement and its heat transfer performance, *Acta Mechanica* 201 (1-4) (2008) 171-184
- [24] He L, Oldfield M L G, Unsteady Conjugate Heat Transfer Modeling, *Journal of Turbomachinery* 133 (3) (2011)
- [25] Alimohammadi S, Dinneen P, Persoons T, et al., Thermal Management Using Pulsating Jet Cooling Technology, *Journal of Physics: Conference Series* 525 (2014)
- [26] Alimohammadi S, Murray D B, Persoons T, Experimental Validation of a Computational Fluid Dynamics Methodology for Transitional Flow Heat Transfer Characteristics of a Steady Impinging Jet, *Journal of heat transfer: Transactions of the ASME* 136 (9) (2014) 091703-1-091703-9
- [27] Sabato M, Fregni A, Stalio E, et al., Numerical study of submerged impinging jets for power electronics cooling, *International Journal of Heat and Mass Transfer* 141 (2019) 707-718
- [28] Anwarullah M, Vasudeva Rao V, Sharma K V, Experimental investigation for

enhancement of heat transfer from cooling of electronic components by circular air jet impingement, *Heat and Mass Transfer* 48 (9) (2012) 1627-1635

[29] Ganatra K A, Singh D, Numerical investigation of effect of semi-circular confinement bottom opening angle for slot jet impingement cooling on heated cylinder, *International Journal of Thermal Sciences* 149 (2020) 17

[30] Langtry R, Menter F. Transition Modeling for General CFD Applications in Aeronautics[C]. 43rd AIAA Aerospace Sciences Meeting and Exhibit, 2005.

[31] Moffat R, Describing the Uncertainties in Experimental Results, *Experimental Thermal and Fluid Science* 1 (1988) 3-17

Table

Table 1 Sources of experimental uncertainties

Sources of uncertainty	errors
Heat flux measurement	0.50%
Systematic error: T-type thermocouples	0.75%
Systematic error: NI DAQ	0.50%
Systematic error: Noike flowmeter	0.50%
Random error: flow rate measurement	1.70%

Figure

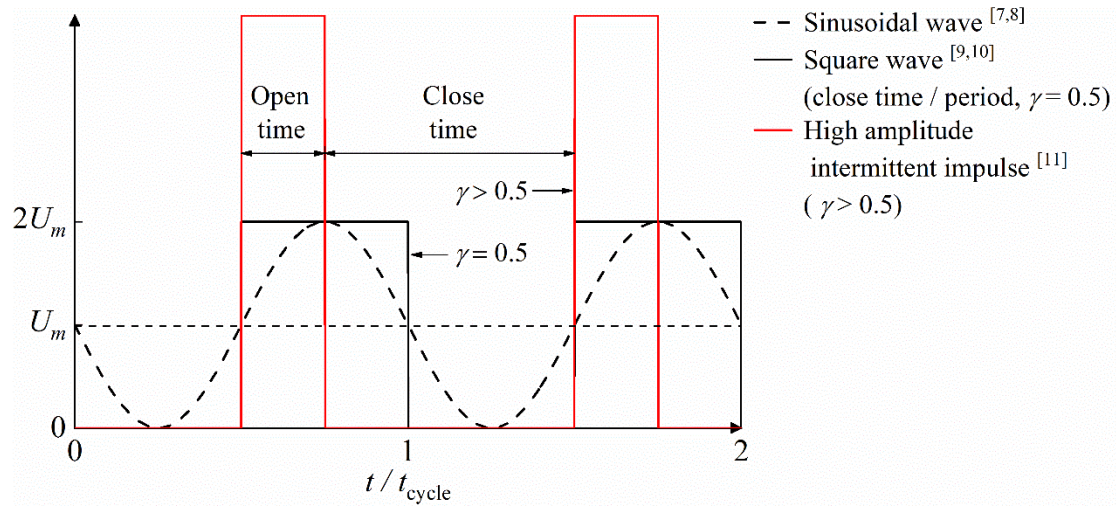


Fig. 1. Different unsteady impingement cooling patterns.

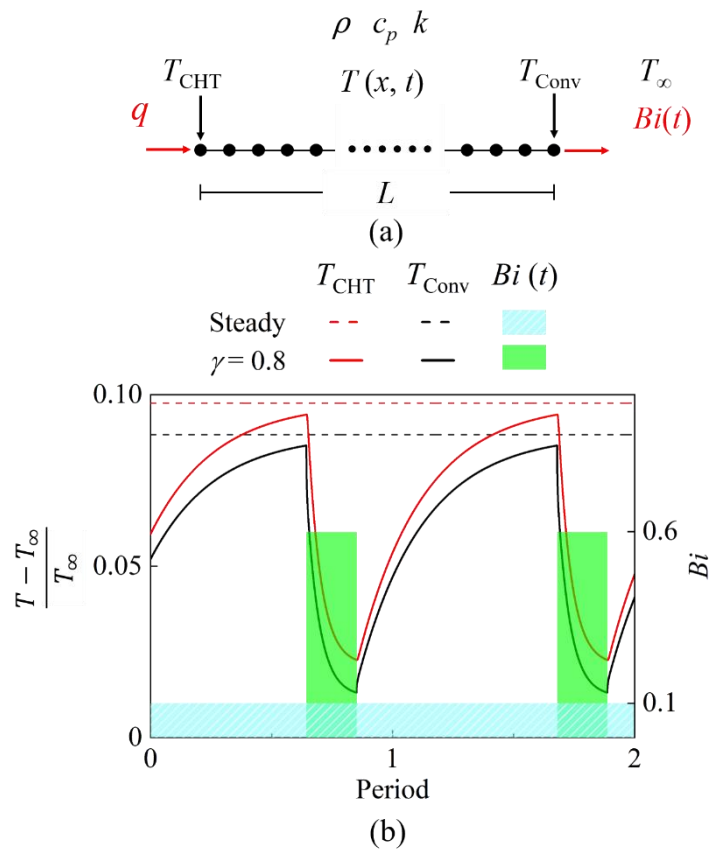


Fig. 2. 1D unsteady conduction analysis: (a) finite difference model; (b) comparison of temperature histories under steady and large close time ratio conditions ($f=0.1$ Hz, $Fo \approx 40$, $\gamma = 0.8$).

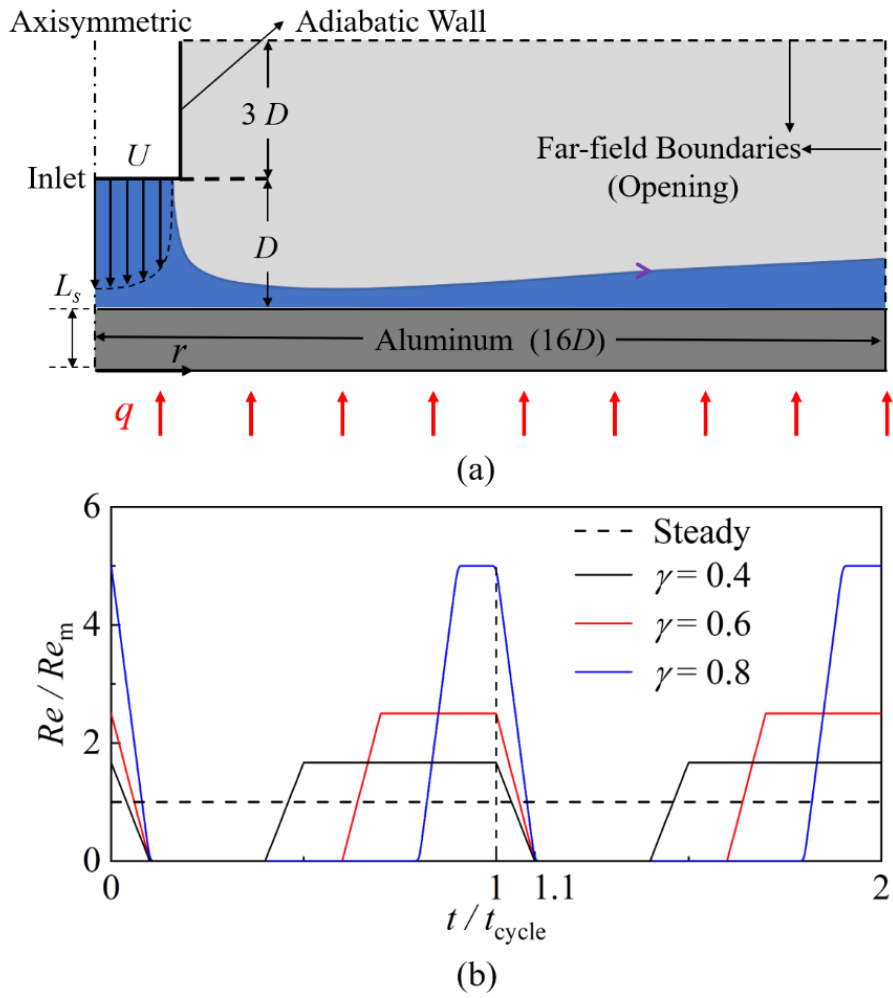


Fig. 3. Computational set up: (a) 2D computational domain; (b) temporal fluctuation history of normalized jet Reynolds number based on the averaged velocity at the inlet.

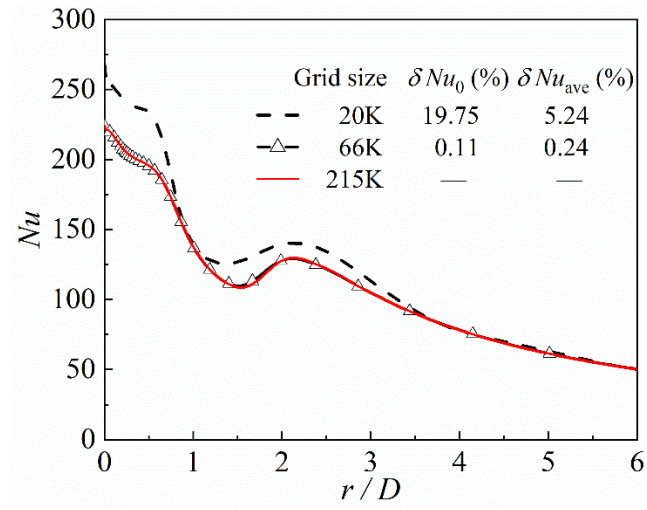


Fig. 4. Grid independence study: Nusselt number variations along radial direction for three different grid sizes.

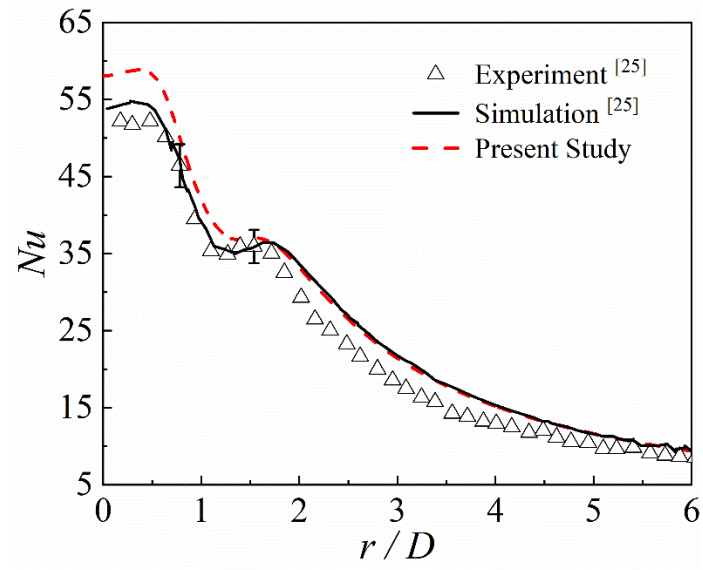


Fig. 5. Comparison of Nusselt number distribution with previous published experimental data^[25] at steady impingement cooling condition ($Re = 6000, Pr = 0.7$).

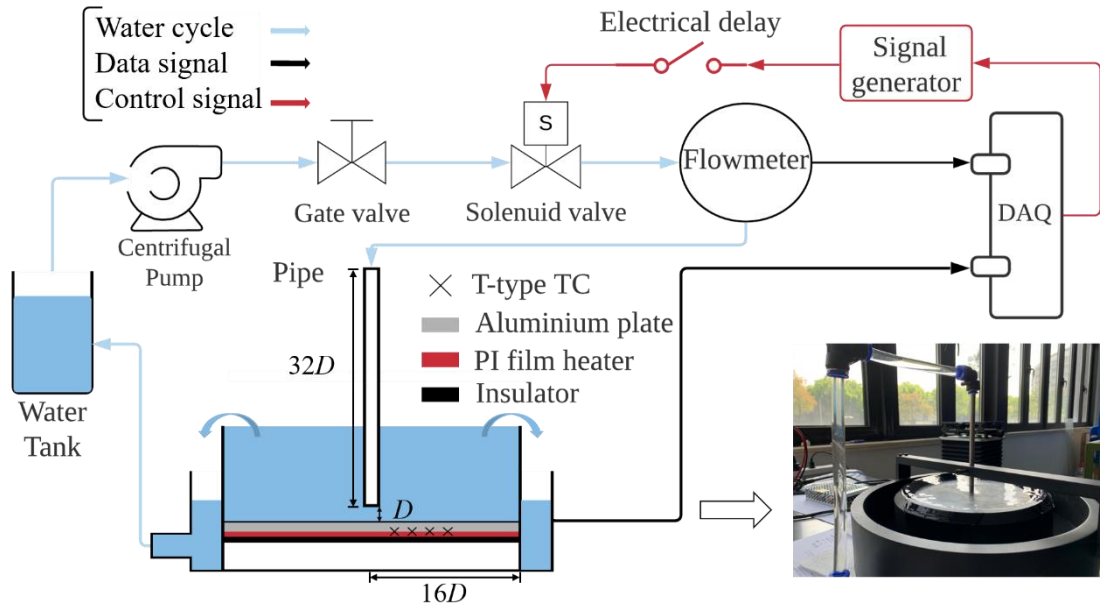


Fig. 6. Experimental setup of intermittent impingement cooling study.

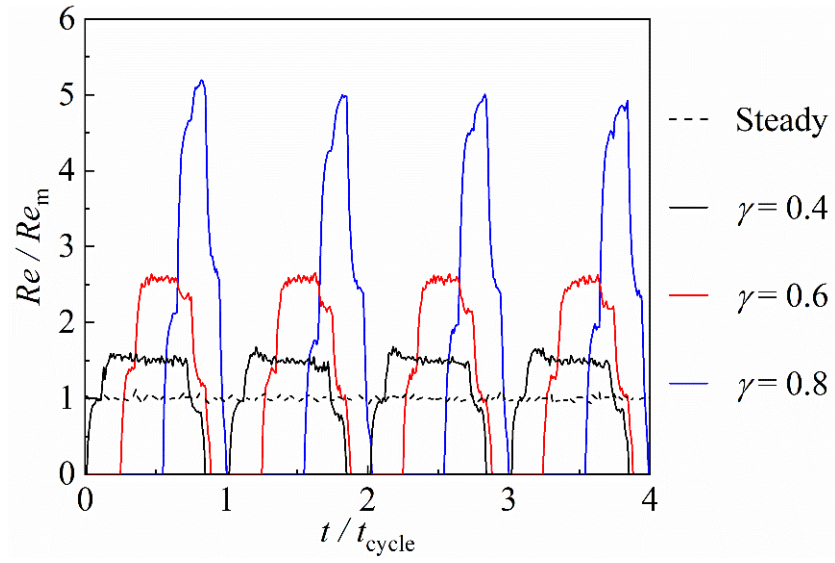


Fig. 7. Temporal distribution of Reynolds number during intermittent impingement cooling experiments ($Re_m = 2800$).

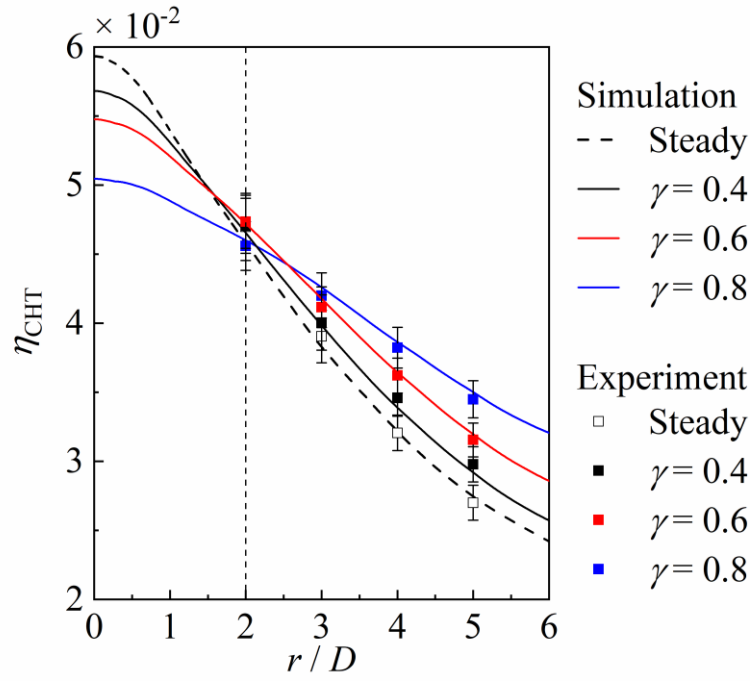


Fig. 8. Comparison of cooling efficiency distributions at different close time ratios ($Re_m = 2800, f = 0.1$ Hz).

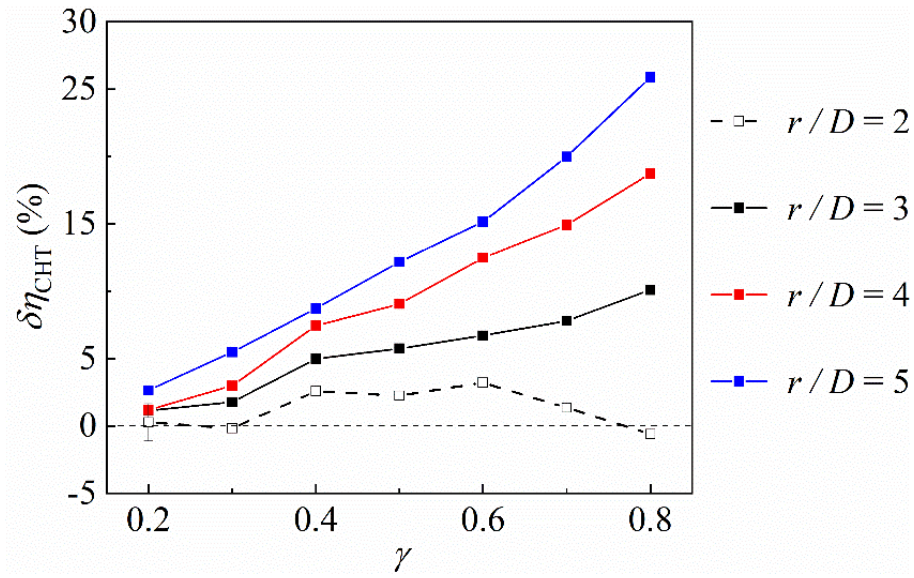


Fig. 9. Percentage difference of local cooling efficiency at four radial locations under various close time ratios ($Re_m = 2800, f = 0.1$ Hz).

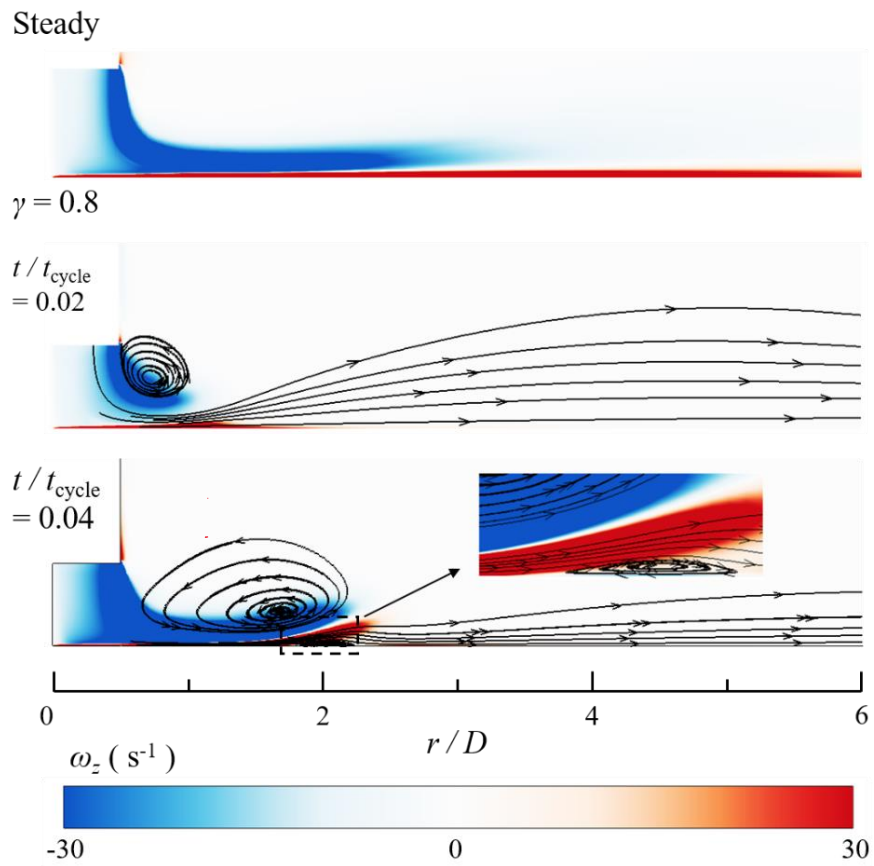


Fig. 10. Comparison of vorticity contours and streamlines under steady condition and intermittent impingement cooling at close time ratio γ of 0.8 ($Re_m = 2800, f = 0.1\text{Hz}, 0 < r/D < 6$).

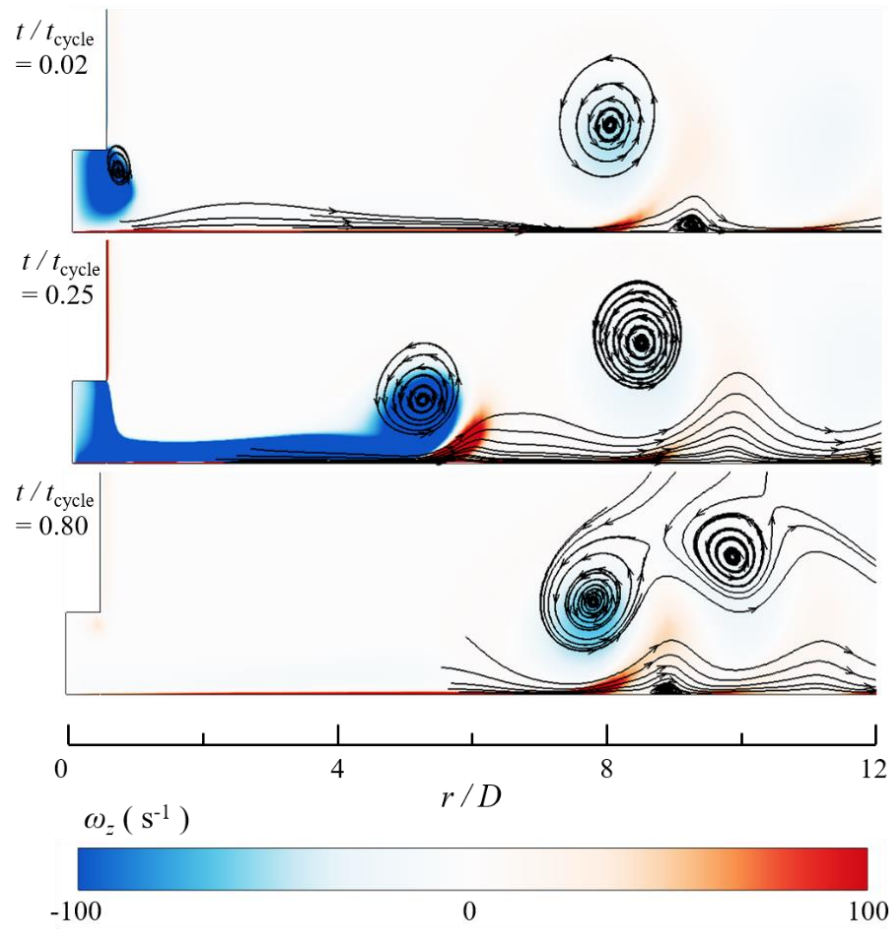


Fig. 11. Near-wall vortex ring merging mechanism illustrated by instantaneous vorticity contours and streamlines at three representative time sequences ($Re_m = 10000$, $f = 2$ Hz, $\gamma = 0.8$).

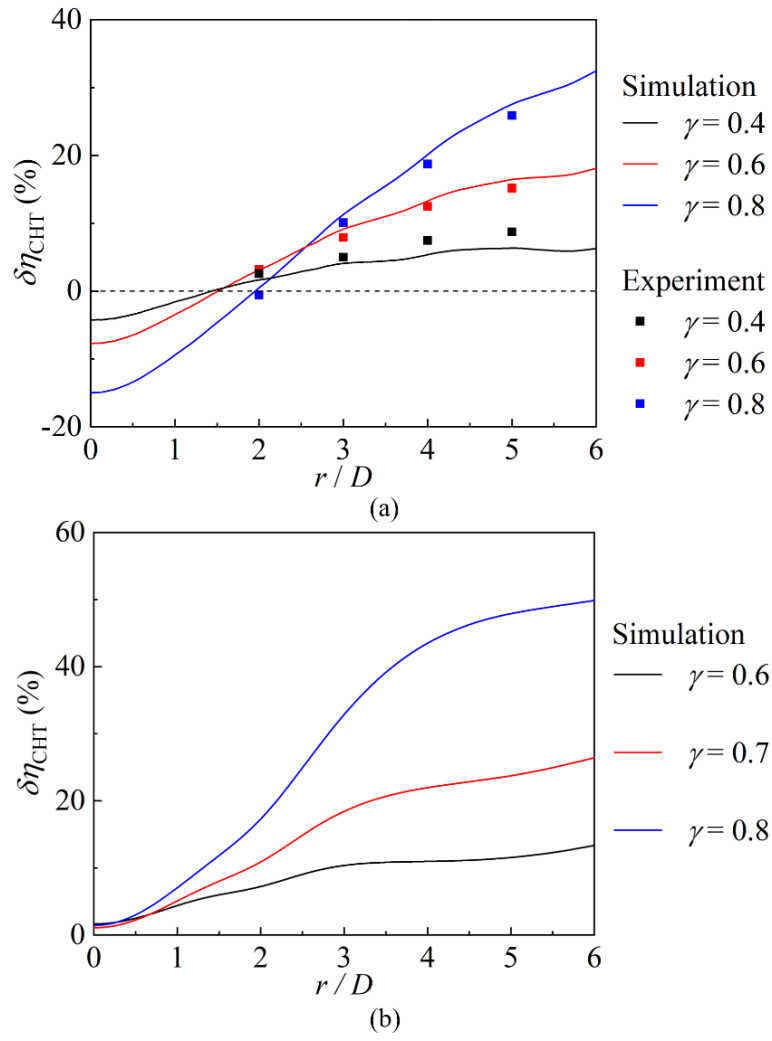


Fig. 12. Percentage increase of cooling efficiency at different close time ratios: (a) $Re_m = 2800, f = 0.1 \text{ Hz}$; (b) $Re_m = 10000, f = 2 \text{ Hz}$.

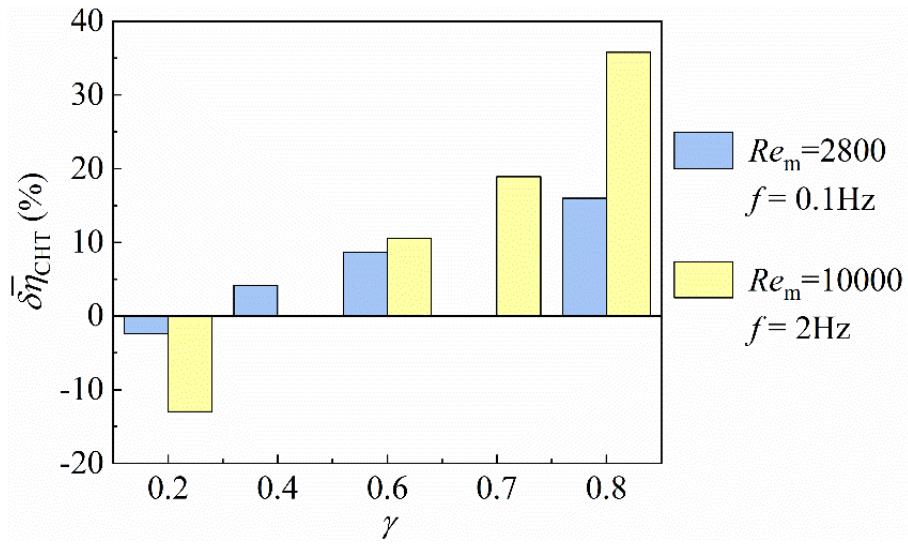


Fig. 13. Total area-averaged integral difference of cooling efficiency at different close time ratios for wall surface $0 < r / D < 6$ ($Re_m = 2800$ and $f = 0.1$ Hz, $Re_m = 10000$ and $f = 2$ Hz)

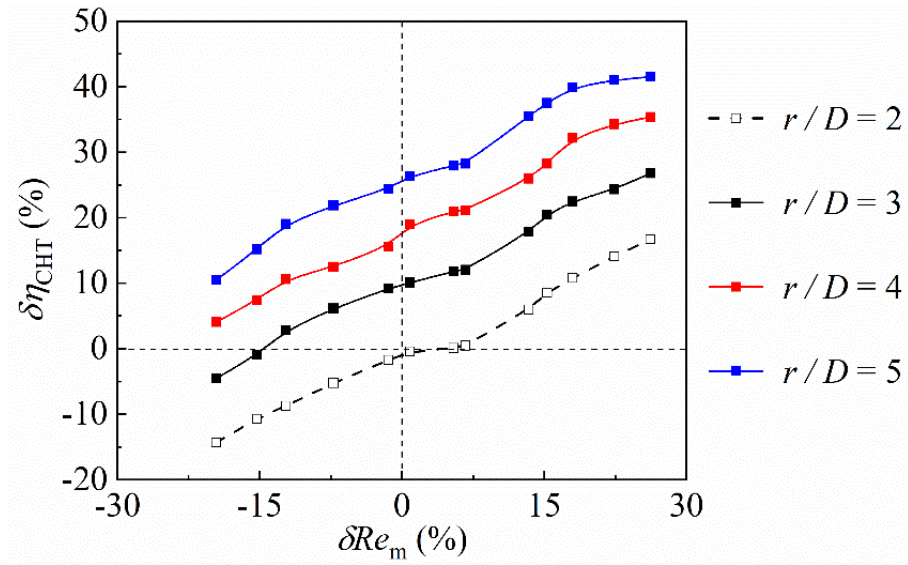


Fig. 14. Experimental data of percentage difference in cooling efficiency at different averaged Reynolds numbers (The benchmark conditions: $Re_m = 2800$, $f = 0.1$ Hz, $\gamma = 0.8$).